

Excitation spectrum and instability of a two-species Bose-Einstein condensate

D. Gordon* and C. M. Savage

*Department of Physics and Theoretical Physics, The Australian National University, Canberra,
Australian Capital Territory 0200, Australia*

(Received 24 February 1998)

We numerically calculate the zero-temperature density profile and excitation spectrum of a two-species Bose-Einstein condensate for the parameters of recent experiments. We find that the ground-state density profile of this system becomes unstable in certain parameter regimes, which leads to a phase transition to a new stable state. This state displays spontaneously broken cylindrical symmetry. This behavior is reflected in the excitation spectrum: As we approach the phase transition point, the lowest excitation frequency goes to zero, indicating the onset of instability in the density profile. Following the phase transition, this frequency rises again. [S1050-2947(98)02408-1]

PACS number(s): 03.75.Fi

I. INTRODUCTION

Following the observation of a two-species Bose-Einstein condensate (BEC) by Myatt *et al.* [1], there has been increased interest in the properties and applications of two-species Bose-Einstein condensates. Theoretically, two-species BECs are interesting because they allow the relative phase between the mean-field wave functions to become manifest, whereas the phase of a single BEC cannot be observed. The original experiment of Myatt *et al.* used the $|F, m_f\rangle = |1, -1\rangle$ and $|2, 2\rangle$ hyperfine sublevels of ^{87}Rb in a cloverleaf trap. The two species formed slightly overlapping clouds that were offset relative to one another by gravity. Recent progress has also been made in the production of two-species BECs in which the two condensates share the same trap center and are therefore less like two separate single condensates [2]. This system uses the $|1, -1\rangle$ and $|2, 1\rangle$ sublevels of ^{87}Rb , which have the same magnetic-dipole moment to first order.

In this paper we consider the quasiparticle, or collective excitation, spectrum of this latter system [3–6]. We find an interesting dependence of the excitation frequencies, which clearly shows the onset of instability in the density profile as particle number is increased and a subsequent phase transition to a stable configuration. This behavior is due to the tendency of the two species to separate out like oil and water in certain parameter regimes [7]. As in the two-dimensional (but nonzero-temperature) calculation of Öhberg and Stenholm [8], our zero-temperature three-dimensional calculations show that this phase transition can take the form of a spontaneous breaking of cylindrical symmetry. The onset of this instability as particle number is increased is indicated by an excitation frequency that goes to zero. Following a phase transition to a stable state, this frequency rises again to a constant value.

Our work builds on previous studies of the excitations and stability properties of two-species BECs. Graham and Walls [3] have analytically solved for the excitations of a binary phase two-species BEC in a trap, in the Thomas-Fermi limit,

and in the case where the parameters satisfy conditions leading to a pure binary phase two-species BEC. Busch *et al.* [4] have performed a variational calculation in which they compute the lowest-lying excitation frequencies. Esry and Greene [5] have numerically calculated the excitation spectrum of a two-species BEC in a time-averaged orbiting potential (TOP) trap in which gravity separates the centers of the two condensates. They found that the repulsive interaction between the two clouds lead to simultaneous collective excitations of both species, which were significantly different from the single-condensate case. However, this system did not display the stability properties presented here. Pu and Bigelow [9,6] have solved for the case of mixed Rb-Na condensate under assumptions of cylindrical symmetry of the density profiles and found that this system also displayed instabilities of the kind presented here; however, they have not investigated the effect of spontaneous breaking of cylindrical symmetry.

II. GROUND-STATE DENSITY PROFILE AND EXCITATION SPECTRUM

For a two-species condensate, the second quantized grand canonical Hamiltonian is, in the position basis,

$$\begin{aligned}
 H = & \int d^3\mathbf{r} \hat{\Psi}_A^\dagger(\mathbf{r}) \left[\frac{\hat{\mathbf{p}}^2}{2m} + V_A(\mathbf{r}) - \mu_A \right] \hat{\Psi}_A \\
 & + \int d^3\mathbf{r} \hat{\Psi}_B^\dagger(\mathbf{r}) \left[\frac{\hat{\mathbf{p}}^2}{2m} + V_B(\mathbf{r}) - \mu_B \right] \hat{\Psi}_B \\
 & + \frac{U_{AA}}{2} \int d^3\mathbf{r} \hat{\Psi}_A^\dagger(\mathbf{r}) \hat{\Psi}_A^\dagger(\mathbf{r}) \hat{\Psi}_A(\mathbf{r}) \hat{\Psi}_A(\mathbf{r}) \\
 & + \frac{U_{BB}}{2} \int d^3\mathbf{r} \hat{\Psi}_B^\dagger(\mathbf{r}) \hat{\Psi}_B^\dagger(\mathbf{r}) \hat{\Psi}_B(\mathbf{r}) \hat{\Psi}_B(\mathbf{r}) \\
 & + U_{AB} \int d^3\mathbf{r} \hat{\Psi}_A^\dagger(\mathbf{r}) \hat{\Psi}_B^\dagger(\mathbf{r}) \hat{\Psi}_A(\mathbf{r}) \hat{\Psi}_B(\mathbf{r}), \quad (1)
 \end{aligned}$$

where $\hat{\Psi}_A(\mathbf{r})$ and $\hat{\Psi}_B(\mathbf{r})$ are the field annihilation operators for species A and B , respectively, $\mu_{A,B}$ are the chemical

*Electronic address: Dan.Gordon@anu.edu.au

potentials for the two species, m is the atomic mass (assumed here to be equal for species A and B), $V_{A,B}$ are the trapping potentials for the two species, and the $U_{AA, BB, AB}$ are the scattering parameters ($U_{pq} = 4\pi a_{pq} \hbar^2/m$, where $a_{AA, BB, AB}$ are the scattering lengths between two atoms of species A , two atoms of species B , and an atom of species A and an atom of species B). Setting $\Psi_A = \psi + \hat{\delta}_A$ and $\Psi_B = \psi + \hat{\delta}_B$, where the $\psi = \langle \hat{\Psi} \rangle$ are c numbers and the $\hat{\delta}$'s contain the operator dependence, we can expand Eq. (1) in the deviation operators $\hat{\delta}_{A,B}$. Assuming that the condensate is approximately in a coherent state allows us to discard the third- and fourth-order terms in the $\hat{\delta}$'s, since these are small. The zeroth-order term in the $\hat{\delta}$'s gives the energy functional, whose stationary points subject to a particle number constraint are given by solutions to the Gross-Pitaevskii equation [10]. The first-order term vanishes if the Gross-Pitaevskii equation is satisfied and the second-order term can be diagonalized with a Bogoliubov transformation, giving the quasiparticle or excitation energies for the BEC.

We use a variation of the well-known basis set method [12] to minimize the energy functional. This method consists in working in a basis of harmonic-oscillator eigenfunctions for the bare trapping potential. We scale these basis vectors appropriately so that the expansion of the condensate due to repulsive atom-atom interactions is partially accounted for. The scaling factors are determined by a variational technique using Gaussian trial wave functions. This allows us to calculate using fewer basis vectors or even, in certain geometries, to accurately scale out the dependence in one or two dimensions.

We define a scaled basis as

$$\phi_i(x, y, z) = (\lambda_x \lambda_y \lambda_z)^{1/2} \Phi_i\left(\frac{x}{\lambda_x}, \frac{y}{\lambda_y}, \frac{z}{\lambda_z}\right), \quad (2)$$

where the $\Phi_i(r)$ are normal modes of the free trap Hamiltonian and the λ 's are scaling factors determined by minimizing the energy functional with Gaussian trial wave functions. We have found that we can generally achieve reasonable accuracy with around 200 basis vectors, although this depends on the geometry of the problem and the parameter regimes explored.

In this basis, the energy functional becomes

$$\begin{aligned} E = & \sum_{i,j} H_{ij}^{0A} \alpha_i \alpha_j + H_{ij}^{0B} \beta_i \beta_j \\ & + \sum_{i,j,k,l} \left(\frac{1}{2} N_A^2 U_{AA} V_{ijkl}^{AA} \alpha_i \alpha_j \alpha_k \alpha_l \right. \\ & \left. + \frac{1}{2} N_B^2 U_{BB} V_{ijkl}^{BB} \beta_i \beta_j \beta_k \beta_l + N_A N_B U_{AB} V_{ijkl}^{AB} \alpha_i \beta_j \alpha_k \beta_l \right), \end{aligned} \quad (3)$$

where the α_i 's and β_i 's are the amplitudes in the various modes for species A and B , respectively, $H_{nm}^{0A,B}$ are the matrix elements of the noninteracting Hamiltonian $p^2/2m + V_{A,B}(r)$ in the expanded basis, and the $V_{ijkl}^{AA, AB, BB}$ are the matrix elements of the two-body potential

$$V_{ijkl}^{pq} = \int d^3r \phi_i^p(r) \phi_j^q(r) \phi_k^p(r) \phi_l^q(r), \quad (4)$$

where p and q denote the species of atom (A or B). The stationary conditions of the energy functional subject to constraints of particle number conservation lead to the Gross-Pitaevskii equations for a two-species condensate [11,4,9].

We determine the ground-state density profile by numerically minimizing the energy functional (3) subject to constant particle number. We do this rather than the more usual and computationally simpler procedure of solving the Gross-Pitaevskii equation since any minimum of the energy functional is a solution to the Gross-Pitaevskii equation, but the set of solutions to the latter also include maxima and saddle points of the energy functional. In the particular case considered here, solutions to the Gross-Pitaevskii equation can become unstable as parameters are varied and we need to take this into account. This instability is a result of the tendency of two-species condensates to form two separate clouds in certain parameter regimes.

The excitation spectrum is then calculated by solving the Bogoliubov equations. In the discrete basis used here, these equations amount to solving the eigenproblem for a non-Hermitian matrix formed from the α 's and β 's. The two-species condensate case generalizes readily from the single condensate case, for which details can be found in [12]. The matrix to be diagonalized has the form

$$\begin{bmatrix} P_{AA} & P_{AB} & -Q_{AA} & -Q_{AB} \\ P_{BA} & P_{BB} & -Q_{BA} & -Q_{BB} \\ Q_{AA} & Q_{AB} & -P_{AA} & -P_{AB} \\ Q_{BA} & Q_{BB} & -P_{BA} & -P_{BB} \end{bmatrix}, \quad (5)$$

where

$$\begin{aligned} P_{ij}^{AA} &= H_{ij}^{0A} - \mu_A + \sum_{k,l} 2U_{AA} V_{ijkl}^{AA} \alpha_k \alpha_l + U_{ikjl}^{AB} \beta_k \beta_l, \\ P_{ij}^{AB} &= \sum_{k,l} U_{AB} V_{ilkj}^{AB} \alpha_k \beta_l, \\ P_{ij}^{BA} &= \sum_{k,l} U_{AB} V_{kijl}^{AB} \alpha_k \beta_l, \\ Q_{ij}^{AA} &= \sum_{k,l} U_{AA} V_{ijkl}^{AA} \alpha_k \alpha_l, \\ Q_{ij}^{AB} &= \sum_{k,l} U_{AB} V_{ijkl}^{AB} \alpha_k \beta_l, \\ Q_{ij}^{BA} &= \sum_{k,l} U_{AB} V_{jikl}^{AB} \alpha_k \beta_l. \end{aligned} \quad (6)$$

P^{BB} and Q^{BB} are defined as for P^{AA} and Q^{AA} , respectively, with $A \leftrightarrow B$ and $\alpha \leftrightarrow \beta$. The various symmetries that exist for given trapping geometries and parameter regimes can be used to simplify the problem by separating the matrix (5) into several smaller matrices.

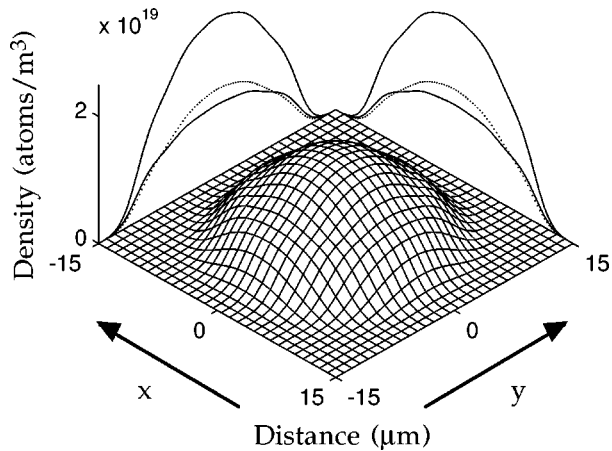


FIG. 1. Radial cross section through the density profile for the parameters $a_{AB}=5.0$ nm and $N_A=N_B=15\,000$ atoms. The cross section is taken through the minimum of the trapping potential in the longitudinal direction. The mesh plot shows the maximum density for species A and B and the line plots show the densities along the x and y axes of the combined density (upper plots) and species A and B densities (solid and dotted lines, respectively). In this case, the scattering length a_{AB} is small enough compared to the two single-species scattering lengths that the two species show no tendency to form separate clouds.

III. RESULTS

We consider here equal trapping potentials for species A and B . This situation has been experimentally achieved for ^{87}Rb atoms in the $|F, M_F\rangle = |1, -1\rangle$ and $|2, 1\rangle$ hyperfine sub-levels, which we label $|A\rangle$ and $|B\rangle$ [2]. We consider trap frequencies of $f_x=f_y=47/\sqrt{8}$ Hz and $f_z=47$ Hz, which are relevant to these experiments in a TOP trap. The low inelastic collision cross section for these species is consistent with scattering lengths $a_{AA, BB, AB}$, which are all similar. Recent calculations give $a_{AA}=5.68$ nm and $a_{BB}=5.36$ nm [13]. We consider the three cases $a_{AB}=5.0, 5.52,$ and 6.0 nm, which are within the range of expected values for this quantity, in order to show the onset of phase instability as a_{AB} is increased.

As shown by Ho and Shenoy [7], a binary condensate in the high particle number (Thomas-Fermi) limit can contain volumes in which only one species is present (giving two single-particle phases, one for each species) and volumes in which both species coexist (binary phase) separated by phase boundaries. As an example, a condensate for which all parameters except the interspecies scattering length are the same for each species will exist as a single binary phase cloud only if $U_{AB} < U_{AA/BB}$. If we discard the Thomas-Fermi assumption, then this single-species phase or binary-phase picture is only approximate since the kinetic-energy term in the Hamiltonian precludes the existence of sharp phase boundaries. However, a two-species BEC can still undergo phase transitions in the sense that a solution to the Gross-Pitaevskii equation may become unstable as parameters are varied and the condensate will then undergo collapse to some other stable solution.

Figure 1 shows a radial cross section through the density profile for $a_{AB}=5.0$ nm and $N_A=N_B=15\,000$ atoms. We see that in this case the two-species condensate exists as two highly overlapping clouds with no tendency to repel each

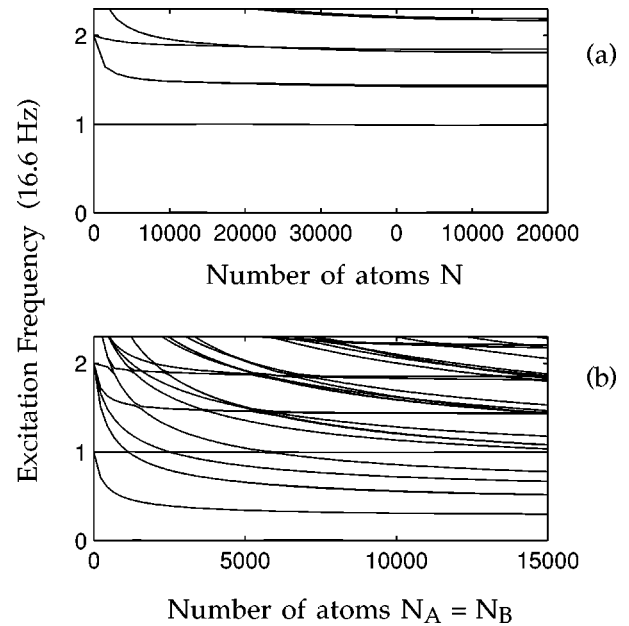


FIG. 2. (a) Excitation spectrum for a single species BEC with $a=5.52$ nm. Parameters were chosen to approximate (b) as closely as possible. (b) Excitation spectrum for the parameters of Fig. 1.

other. The corresponding excitation spectrum is shown in Fig. 2(b), and Fig. 2(a) shows a single-species condensate with $a = \sqrt{a_{AA}a_{BB}}$. We see that, as predicted by Graham and Walls [3], the excitation spectrum of the two-species condensate undergoes a doublet splitting as compared to the case of a single-species condensate. We have compared our results to the high atom number limit derived by Graham and Walls for a spherically symmetric two-species condensate and found agreement to within a few percent with less than 200 basis vectors.

Figure 3 shows what happens when a_{AB} is increased to $\sqrt{a_{AA}a_{BB}}=5.52$ nm. We see that at high atom number, the lowest-energy eigenvalue approaches closer to zero frequency than in the case of Fig. 2, suggesting that we are near a region of phase instability in parameter space.

Indeed, in the case $a_{AB}=6.0$ nm, the single-phase solution to the Gross-Pitaevskii equation becomes unstable at a critical atom number of around 4000. The minimum of the energy functional is given by a different density profile, as shown in Fig. 4. It can clearly be seen that the cylindrical

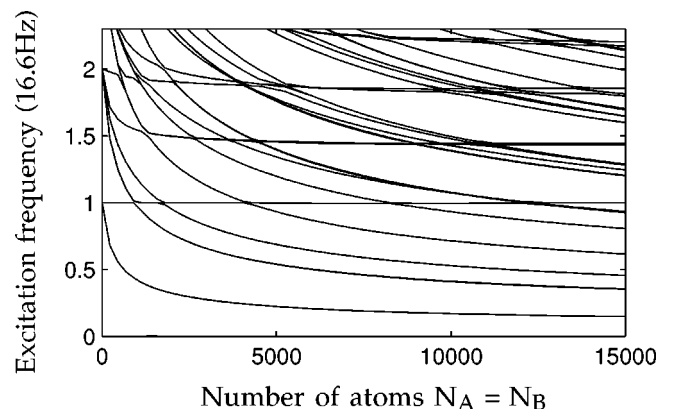


FIG. 3. Excitation spectrum for $a_{AB}=5.52$ nm.

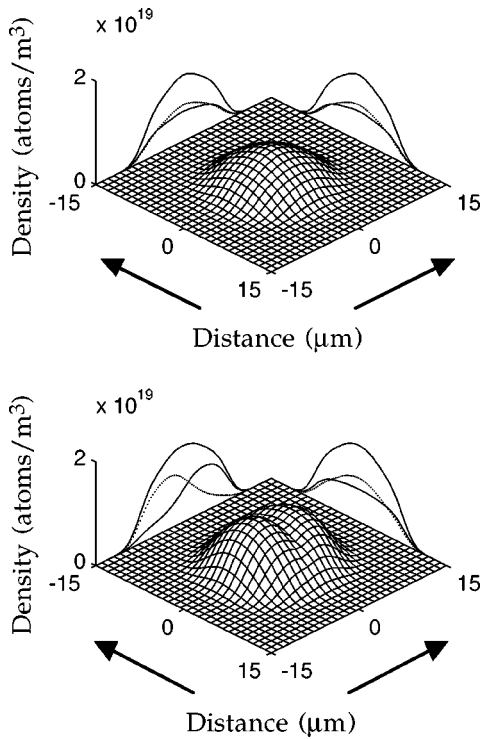


FIG. 4. Density profile for $a_{AB}=6.0$ nm. The top plot shows the densities for $N=3000$ and the bottom plot shows the densities for $N=4500$. The spontaneous breaking of cylindrical symmetry is seen in the latter case.

symmetry is spontaneously broken by the two condensates' mutual repulsion. This effect was also seen by Öhberg and Stenholm [8] in a two-dimensional calculation. It illustrates the danger in assuming spherical or cylindrical symmetry when solving for the density profile of a binary condensate, since in this case such an assumption leads to a state that is unstable with respect to certain antisymmetric perturbations.

The excitation spectrum for the parameters of Fig. 4 is shown in Fig. 5. We can clearly see that, for low atom numbers, the lowest (antisymmetric) excitation frequency goes to zero, suggesting the increasing instability of the condensate to antisymmetric perturbations. This is indeed the case, as is shown by the breaking of cylindrical symmetry seen in Fig. 4. When $N \approx 4000$ is reached, the condensate undergoes a phase transition to an unsymmetric ground state and the lowest-energy eigenvalue increases again to an asymptotic limit.

One further interesting feature of this excitation spectrum is the persistence of excitations that look like the single-condensate case even after the phase transition is reached, for example, the nearly horizontal excitation at 16.6 Hz, which

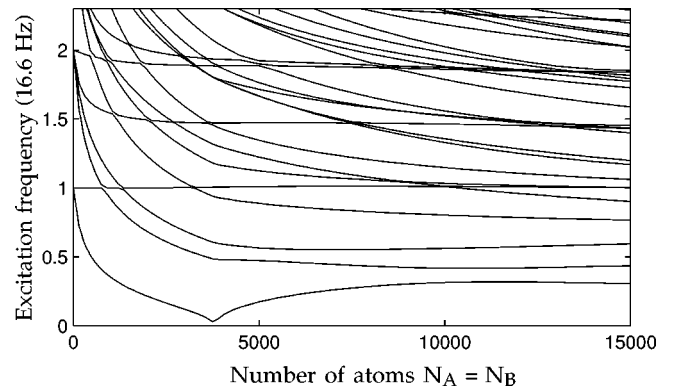


FIG. 5. Excitation spectrum for $a_{AB}=6.0$ nm. The onset of phase instability can be seen at around $N=4000$ and is characterized by the lowest excitation frequency approaching zero. Following a phase transition to a symmetry-broken state, the lowest-energy eigenvalue increases again, tending towards an asymptotic limit.

is hardly modified after the phase transition point. We interpret this as being due to the fact that, in the region above the phase transition, the *combined* density profile of the two species looks very much like a single-species condensate, even though the individual density profiles of each species are greatly modified (see Fig. 4). The excitations in question are then interpreted as the normal single-species type of excitations for this combined density profile.

IV. CONCLUSION

In certain parameter regimes, two-species Bose-Einstein condensates can show more complex density profile behavior than single condensates. In particular, solutions to the Gross-Pitaevskii equation can become unstable or metastable as parameters are adiabatically changed, leading to different ground-state solutions. We have examined the way this effect shows up in the excitation spectra of experimentally realistic two-species condensates and found that the onset of instability is heralded by an excitation frequency that tends to zero, as would be expected. The nature of the instability is consistent with the parity of the corresponding excitation.

Note added in proof. Recently, Hall *et al.* has given a value of the scattering length $a_{AB}=5.5(3)$ nm (D. S. Hall, M. R. Matthews, J. R. Ensher, C. E. Wieman, and E. A. Cornell, e-print cond-mat/9804138).

ACKNOWLEDGMENTS

The authors would like to thank Michael Matthews for discussions of current experiments. The calculations were performed at the Australian National University Supercomputer Facility. This work was supported by the Australian Research Council.

- [1] C. J. Myatt, E. A. Burt, R. W. Ghrist, E. A. Cornell, and C. E. Wieman, Phys. Rev. Lett. **78**, 586 (1997).
 [2] M. R. Matthews, D. S. Hall, D. S. Jin, J. R. Ensher, C. E. Wieman, E. A. Cornell, F. Dalfovo, C. Minniti, and S. Strin-

- gari, e-print cond-mat/9803310; D. S. Hall, M. R. Matthews, J. R. Ensher, C. E. Wieman, and E. A. Cornell, e-print cond-mat/9804138; D. S. Hall, M. R. Matthews, C. E. Wieman, and E. A. Cornell, e-print cond-mat/9805327.

- [3] R. Graham and D. F. Walls, *Phys. Rev. A* **57**, 484 (1998).
- [4] Th. Busch, J. I. Cirac, V. M. P eres Garc ıa, and P. Zoller, *Phys. Rev. A* **56**, 2978 (1997).
- [5] B. D. Esry and Chris H. Greene, *Phys. Rev. A* **57**, 1265 (1998).
- [6] H. Pu and N. P. Bigelow, *Phys. Rev. Lett.* **80**, 1134 (1998).
- [7] T. L. Ho and V. B. Shenoy, *Phys. Rev. Lett.* **77**, 3276 (1996).
- [8] Patrik  hberg and Stig Stenholm, *Phys. Rev. A* **57**, 1272 (1998).
- [9] H. Pu and N. P. Bigelow, *Phys. Rev. Lett.* **80**, 1130 (1998).
- [10] E. M. Lifshitz and L. P. Pitaevskii, *Statistical Physics Part 2* (Pergamon, Oxford, 1980).
- [11] B. D. Esry, C. H. Greene, J. P. Burke, Jr., and J. L. Bohn, *Phys. Rev. Lett.* **78**, 3594 (1997).
- [12] Mark Edwards, R. J. Dodd, and Charles W. Clark, *J. Res. Natl. Inst. Stand. Technol.* **101**, 553 (1996).
- [13] M. Matthews (unpublished), and private communication.